HHS Public Access

Author manuscript

Head Neck. Author manuscript; available in PMC 2015 April 20.

Published in final edited form as:

Head Neck. 2008 June ; 30(6): 782–789. doi:10.1002/hed.20782.

FLUORESCENT LABELED ANTI-EGFR ANTIBODY FOR IDENTIFICATION OF REGIONAL AND DISTANT METASTASIS IN A PRECLINICAL XENOGRAFT MODEL

John P. Gleysteen, BS[1], **J. Robert Newman, MD**[1], **David Chhieng, MD**[2], **Andra Frost, MD**[2], **Kurt R. Zinn, DVM, PhD**[3], and **Eben L. Rosenthal, MD**[1]

[1]Department of Surgery, Division of Otolaryngology–Head and Neck Surgery, University of Alabama at Birmingham, Birmingham, Alabama. oto@uab.edu

[2]Department of Pathology, University of Alabama at Birmingham, Birmingham, Alabama

[3]Department of Medicine, University of Alabama at Birmingham, Birmingham, Alabama

Abstract

Background—Detection of regional and distant metastatic disease has significant implications for patient management. Fluorescent imaging may be a useful technique for metastasis detection and removal.

Methods—Anti–epidermal growth factor receptor antibody (cetuximab) and isotype-matched control antibody (immunoglobulin G [IgG]) were labeled with a near-infrared fluorophore (Cy5.5), then systemically administered to mice with tumors resulting from either intraoral or intravenous injections of head and neck squamous cell carcinoma. Mice were sacrificed before undergoing fluorescent stereomicroscopy to assess pulmonary or cervical lymph node metastasis. Fluorescent areas were serially excised until wound bed demonstrated negative fluorescence.

Results—Mice bearing pulmonary metastases displayed diffuse background after IgG–Cy5.5 injection, but demonstrated a speckled fluorescent pattern across lung surface following cetuximab–Cy5.5 injection. Mice bearing cervical metastases demonstrated clear fluorescence of primary tongue tumor and bilateral cervical nodes. Fluorescence correlated with histopathology.

Conclusion—These data suggest that cetuximab–Cy5.5 may have clinical utility in the detection and guided the removal of regional and distant micrometastasis.

Keywords

anti-EGFR antibody; optical imaging; fluorescence; metastasis detection; head and neck cancer

Detection of regional and distant metastatic disease has significant implications for patient management. The vast majority of distant metastasis in head and neck squamous cell carcinoma (HNSCC) occurs in the chest and, when present, is a contraindication to surgical therapy. Development of regional metastasis from HNSCC is associated with a 50%

Correspondence to: E. L. Rosenthal.

reduction in patient survival.[1] Complete removal of cervical lymph nodes is performed in patients with head and neck cancer for prognostic and therapeutic reasons; however, cervical lymphadectomy is associated with significant morbidity and operative time. Noninvasive imaging modalities used for detecting metastatic disease are CT, MR, and ^{18}F-fluoro-deoxy-glucose positron emission tomography (FDG PET). The most sensitive and specific modality of imaging pulmonary metastasis is currently performed by PET-CT imaging, followed by lung or mediastinal lymph node biopsy.[2] Unfortunately, these modalities cannot be used in real time to guide surgical resection or biopsy. Furthermore, unlike many radiological techniques, optical imaging allows simultaneous viewing of the anatomical surface and the fluorescent image in real time. Accurate detection and pathologic confirmation of metastatic disease during surgical procedure may improve patient outcomes by promoting minimally invasive procedures.

The coupling of fluorescent dyes to tumor-specific probes for the purposes of optical imaging is a rapidly emerging imaging modality because of its high sensitivity and spatial resolution.[3,4] The selective property of therapeutic antibodies for tumor cells makes this an optimal method for imaging. Epidermal growth factor receptor (EGFR) is overexpressed in 80% to 90% of head and neck cancers and is upregulated during the early stages of tumor development.[5,6] Cetuximab (Erbitux, ImClone Systems, Branchburg, New Jersey) is a therapeutic antibody directed against EGFR and approved for treatment of head and neck cancer.[7] We hypothesize that fluorescently labeled cetuximab would localize in small islands of pulmonary or cervical metastasis due to the abundance of EGFR in HNSCC compared with the surrounding normal cells. We hypothesize that this technique can detect and guide the removal of regional and distant metastatic disease.

We have previously demonstrated that the fluorescently labeled antibody is specific to head and neck cancer xenografts in a preclinical murine model.[8–10] The purpose of this study is to determine if the fluorescently labeled cetuximab could be used in head and neck cancer to detect metastatic disease. To address feasibility of this hypothesis, we assessed fluorescence imaging of metastatic head and neck cancer in the lung and neck in a preclinical murine model.

MATERIALS AND METHODS

Cell Lines and Tissue Culture

Two human tumor cell lines were studied: HNSCC (SCC-1; Thomas Carey, University of Michigan, Ann Arbor, Michigan) and oral squamous cell carcinoma (OSC-19; Jeffrey Myers, The University of Texas M. D. Anderson Cancer Center, Houston, Texas). The cells were obtained, grown, and maintained in Dulbecco's modified Eagle's medium (DMEM) containing 10% fetal bovine serum (FBS) and supplemented with L-glutamine, penicillin, and streptomycin. The cells were incubated at 37°C in 5%CO_2.

Reagents

We used cetuximab (ImClone Systems, Branchburg, New Jersey), a recombinant, human/mouse chimeric monoclonal antibody that binds specifically to the extracellular domain of

the human EGFR. Cetuximab is composed of the Fv regions of a murine anti-EGFR antibody with human immunoglobulin G1 (IgG1) heavy and kappa light chain constant regions and has an approximate molecular weight of 152 kDa. Cy5.5 (CyDye deoxynucleotides, GE Healthcare, Piscataway, New Jersey) was used as the far-red fluorescent marker. Cy5.5 has a broad absorption peak with its maximum at 683 nm. Its emission maximum when coupled to IgG is at 707 nm, with a relative quantum yield of .28. Cy5.5 has a degree of labeling of 4.2 moles of dye per mole of protein using an ε of 250,000 M^{-1} cm^{-1} at the absorbance maximum. The molar ratio of dye to protein was confirmed by mass spectrometry prior to injection of the conjugate (data not shown). Cetuximab was labeled according to the manufacturer's instructions. Briefly, cetuximab was incubated with Cy5.5 reactive dye in .15*M* phosphate buffer (pH 7.8) for 1.5 hours. The nonconjugated Cy5.5 was removed by Centricon Centrifugal Filter Unit, YM-30 (Millipore, Billerica, Massachusetts). Human IgG1k antibody (Alexis Biochemicals, San Diego, California) was used as an isotype matched control antibody (MW, 146 kDa). All procedures were conducted under aseptic technique.

Animal Models

Severe combined immunodeficiency (SCID) male mice, aged 4 to 6 weeks (Charles River Laboratories, Wilmington, Massachusetts), were obtained and housed in accordance with our Institutional Animal Care and Use Committee (IACUC) guidelines, and all experiments were conducted and the animals euthanized according to our institution's IACUC guidelines.

For the pulmonary metastatic model, SCID mice ($n = 8$) received systemic tail vein injections of 2×10^6 SCC1 cells. Two SCID mice were administered injections of 1×10^6 cells to compare the extent of tumor growth and the resulting fluorescence. The cells were prepared in a suspension of 50 μL of media, then diluted to 200 μL with saline. Eleven days after injection of tumor cells, mice ($n = 8$) received a 50 μg dose of the cetuximab–Cy5.5 conjugate so that the dye would have been in circulation for 72 hours prior to imaging on day 14. To detect nonspecific uptake, mice ($n = 2$) received a 50-μg dose of the isotype control IgG1–Cy5.5 conjugate for use as negative controls. Additionally, control mice ($n = 2$) received no tumor cell injection but were given a 50-μg dose of the cetuximab–Cy5.5 conjugate. On day 14, the lungs were removed from the chest to minimize background fluorescence and placed in a dish on a black background. Brightfield and fluorescent images were obtained for each lung individually. The lungs were then paraffin embedded, hematoxylin-eosin (H&E) stained, and placed on slides for pathologic examination.

For a model of regional metastasis, SCID mice ($n = 8$) received injections of 2×10^5 OSC-19 cells suspended in 25 μL of media into the side of their tongue using a 27-gauge insulin syringe, as previously described.[11] After 14 days, mice ($n = 6$) received a 50-μg dose of the cetuximab–Cy5.5 conjugate. To measure the nonspecific uptake, the other 2 mice received a 50-μg dose of the isotype control IgG1–Cy5.5 conjugate. One additional control mouse was not injected with tumor cells but received a 50-μg dose of the cetuximab–Cy5.5 conjugate. After 72 hours of the injection of the labeled antibody, each mouse was sacrificed and placed on its back with arms outstretched and pinned down. A skin incision was made

from the rib cage to the chin and the cervical skin was removed, then bright field and fluorescent images (at 800- and 200-ms exposure) of the neck were taken. Bright fluorescent spots were excised until the fluorescence disappeared. Each sample was then fixed, H&E-stained, and placed on slides. Biopsies of the tongue (primary tumor) were also collected for pathological analysis.

Imaging

Fluorescent stereomicroscope imaging was performed with a custom-built Leica fluorescent stereomicroscope (Leica MZFL3 Stereo research microscope. Leica Microsystems, Bannockburn, Illinois) fitted with a Cy5.5 filter and an ORCA ER charge coupled device camera (Hamamatsu, Bridgewater, New Jersey) to allow for real-time imaging of Cy5.5 fluorescence. A Cy5.5 filter (Chroma filter set 41023) provided excitation between 630 and 670 nm and emission measured at 685 to 735 nm. Brightfield and fluorescent images were obtained for each data point.

Immunohistochemistry

Immunostaining for cytokeratin to confirm the presence of tumor was performed using a semi-automated machine (Benchmark XT, Ventana Medical Systems, Tucson, Arizona). Five-micrometer sections were obtained from the paraffin blocks and pretreated by incubating with protease for 4 minutes. Immunostaining was performed using a modified streptavidin-biotin-HRP (horseradish peroxidase) technique. The sections were incubated with an antibody that binds to a mouse monoclonal antibody targeting low-molecular-weight cytokeratin (clone: AE1, prediluted, Ventana, Tucson, Arizona) for 16 minutes at 37°C. The chromogen diaminobenzidine tetrachloride was used to visualize the antibody–antigen complex. Appropriate negative controls, consisting of tissue sections of each case processed without the addition of primary antibody, were prepared along with positive tissue control sections. After immunostaining, the slides were counter-stained with hematoxylin, dehydrated in graded alcohols, and mounted under coverslips. Positive staining was defined by the presence of strong cytoplasmic staining.

Measurement

Fluorescence intensity (luminosity) was measured by drawing a region of interest over sections of the tumors to make a histogram using ImageJ software as previously described.[8] The range of fluorescence intensity was set from 0 to 85 in arbitrary units (au).

Statistical Analysis

Continuous variables (eg, fluorescence) were compared by unpaired *t* test. Data analysis was done using GraphPad Prism software (GraphPad Software, San Diego, California). $p < .05$ was considered significant in unpaired *t* test analysis.

RESULTS

Pulmonary Metastases Demonstrate Fluorescence

Stereomicroscopic imaging of murine lungs in the absence of tumor after injection of cetuximab–Cy5.5 demonstrated diffuse background fluorescence, as shown in the representative images in Figures 1A and 1B. Two weeks after the systemic tail vein injection of SCC1 cells, the fluorescently labeled isotype control antibody or cetuximab (50 μg) was systemically administered by tail vein injection. A diffuse fluorescence on stereomicroscopic imaging was found for the Cy5.5-labeled control antibody (Figures 1D and 1E). In contrast, fluorescent stereomicroscopic imaging after cetuximiab–Cy5.5 injection demonstrated a distinct speckled fluorescence pattern across the surface of the lung. Mice received 2 different doses of tumor cells (1×10^6 and 2×10^6 SCC1 cells) to determine whether increased pulmonary tumor burden positively correlated with elevated numbers of micrometastasis (Figures 1H and 1K). Histological analysis was used to confirm the presence of micrometastatic lesions (Figures 1F, 1I, and 1L). To confirm that areas of fluorescence represented micrometastatic disease, a 2-mm biopsy was obtained from an area of fluorescence in the lung apex (Figure 2); histological analysis confirmed islands of tumor cells within the lung parenchyma (Figure 2C).

Cervical Metastases are Visible by Fluorescence

Two weeks after the intraoral injection of OSC-19 cells, tongue tumors developed and were detectable by inspection and palpation. After systemic injection of cetuximab–Cy5.5 (50 μg) the stereomicroscopic imaging demonstrated bright fluorescence outlining the primary tumor (Figures 3A and 3B). After resection of the overlying skin, cervical lymph nodes were not detectable by gross examination or by bright field stereomicroscopy, but became clearly visible using fluorescence (Figures 3D and 3E). Biopsies were obtained from fluorescent areas and histological analysis of the tongue and the cervical biopsies confirmed the presence of squamous cell carcinoma (Figures 3C and 3F).

When a dose of cetuximab–Cy5.5 was given to a mouse in the absence of tumor, low-level background fluorescence was observed, but cervical lymph nodes were not visualized (Figures 4A and 4B). To show that the fluorescence was due to specific binding of the cetuximab–Cy5.5 to the EGF receptor, we imaged an isotype-matched IgG1–Cy5.5 under the same experimental conditions. The tongue demonstrated nonspecific background fluorescence distributed evenly across the surface, unlike the cetuximab–Cy5.5 (Figures 4C and 4E). When the cervical skin was removed, the lymph nodes demonstrated some fluorescence, which was significantly less intense than seen with the cetuximab–Cy5.5 (Figures 4D and 4F). The mean fluorescence intensity of the cervical lymph nodes after isotype-matched IgG–Cy5.5 was 24.7 ± 4.98 au and cetuximab–Cy5.5 was 38.6 ± 8.09 au. This difference was found to be statistically significant ($p = .0005$).

The tumor fluorescence was used to guide surgical biopsies. Cervical tissues were exposed 2 weeks after tongue injection of tumor cells and 3 days after systemic administration of cetuximab–Cy5.5 in 8 mice. Using fluorescent guidance, biopsies were taken using 2-mm cupped forceps until there was no detectable fluorescence. Histological analysis correlated

fluorescence with the presence of tumor (Figure 5) in all the 8 mice. Biopsies ranged in size from .2 to 2 mm (data not shown). Because the metastatic tumor volume was small and could not be accurately assessed by pathology alone, we performed immunohistochemical analyses of lymph node sections using cytokeratin AE1 antibody. Two pathologists (AF, DC) could confirm the presence of tumor after cytokeratin staining.

DISCUSSION

This study demonstrates the potential to detect micrometastasis in the lungs and cervical lymph nodes using a fluorescently labeled EGFR antibody in a preclinical model. From our pulmonary model of distant metastasis, we showed that the Cy5.5-labeled anti-EGFR antibody will bind specifically to small islands of tumor cells in the lung parenchyma and fluoresced in a distinct miliary pattern, whereas the isotype control IgG just demonstrated diffuse background fluorescence. The mice given half the dose of tumor cells showed a smaller number of fluorescent spots on the lung, and the histology confirmed a lesser degree of disease. We have performed experiments with as few as 200,000 SCC1 cells systemically injected and obtained similar results (data not shown), indicating that there is a low threshold of tumor detection. In our cervical node model of regional metastasis, we demonstrated that this technique allows visualization of the tumor containing node. We showed a nodal biopsy of metastatic disease could be performed under fluorescent guidance and correlated fluorescence to pathologic histology. Fluorescent imaging allowed accurate visualization of nodes in mice that were not detectable by gross palpation. Because of the murine cervical lymph nodes' small size (range, .3–1.5 mm) they were not detectable by gross examination or during surgical exploration using ambient light. In fact, the biopsies were directed on the basis of near-infrared imaging. Although the exact threshold for tumor that this technique can visualize is unknown, tumor at the microscopic level could be detected, which is a significant improvement over current intraoperative methods. In our previous experiments using primary tumors, we were able to demonstrate a specificity of 100% and sensitivity of up to 91%, in which microscopic clusters of tumor cells measuring <450 cells could not be detected.[10]

Optical imaging technology with cancer-specific contrast agent has tremendous implications for assisting clinicians and surgeons in diagnoses and resections as a result of its real-time feedback regarding tumor location and extent. Although the labeling of antibodies with optical markers has been in use for years, recent advancements in the field of fluorescence technology have made the transition of this research into the clinic more feasible now than ever. Recent trends in surgery have stressed minimally invasive procedures that use rigid endoscopes, limit the surgeon's tactile feedback, and are performed in cavities with limited ambient light. These are the ideal conditions for optical imaging, because ambient light can flood the fluorescent probe, and endoscopes fitted with the appropriate filters are ideal to deliver near-infrared images to the surgeons. This technology could be used to safely guide biopsy of pulmonary metastasis or perform a minimally invasive cervical lymph node dissection or biopsy. Although not addressed in the current study, we have previously shown that fluorescently labeled cetuximab is specific for primary tumors and demonstrates significantly higher fluorescence compared with human epithelial background (xenografted

human skin grafts).[8] These results suggest that this technology could be used to facilitate transoral laser or robotic cases for primary tumors.

Previous authors have demonstrated the utility of fluorescently labeled antibodies in a murine xenograft model to successfully detect primary tumors.[12] Our current work builds upon these early optical imaging studies and our previous work by using fluorescently labeled anti-EGFR antibodies to detect micrometastasis. Because EGFR is highly overexpressed in head and neck cancer, it is an optimal target for tumor-specific imaging. Radiolabeled anti-EGFR has been successfully used to localize tumors in similar animal models[13]; however, unlike that modality, optical imaging would allow clinicians to anatomically localize cancer when it is in a smaller size and in the absence of radioactive material. Weissleder et al have had success visualizing tumors using autoquenched near-infrared fluorescence probes activated by tumor-associated lysosomal protease activity.[14] Yet, because of the nonspecific accumulation of the probe in environments with increased vascular permeability and blood flow, inflammatory conditions not associated with cancer could cause a similar response.

Fluorescence imaging has been used previously in clinical settings. Recently, there have been clinical imaging studies using the FDA-approved dye indocyanine green (ICG) for detection of sentinel lymph nodes in patients with gastric,[15] intrathoracic,[16,17] and lung cancer.[18] Surgical oncologists are currently investigating mapping regional metastasis by fluorescent optical imaging using ICG, noncovalently bound to human serum albumin.[19] However, the albumin remains nonspecific for cancer. Unlike these current intraoperative techniques for sentinel lymph node mapping, optical imaging with a cancer-specific probe promises to identify the actual location of tumor at the primary site or metastatic site, rather than identify the lymph node where tumor might metastasize. Furthermore, sentinel lymph node mapping cannot tell the surgeon at the time of the operation whether the cancer is there or if it has been successfully removed; optical fluorescence with a cancer-specific agent may provide real-time information for both.

Neurosurgeons have used near-infrared fluorescence for intraoperative assessment of tumor margins in glioblastomas and verified their findings with postoperative MRI.[20] Their probe was preferentially taken up by tumor but not by the normal neural tissue. Recent preclinical investigations have identified chlorotoxin labeled with Cy5.5 as a potential method for imaging brain tumors intraoperative to determine surgical margins.[3] However, unlike the current study, these authors and others[4] exploring optical contrast agents for clinical translation have used small animal imaging techniques (eg, the IVIS-100 system, eXplore Optix, Kodak in vivo imaging system) to demonstrate feasibility. However, these recent publications suggest a growing enthusiasm for optical imaging as an emerging technology with high clinical potential for surgeons.[3,4,21–24]

Several obstacles to optical imaging in a clinical setting do exist. Although cetuximab is FDA approved for use in humans, the fluorophore Cy5.5 is not. ICG is similar in molecular structure and is used in gram quantities in humans without known toxicity. Unfortunately, ICG is not easily conjugated to proteins and it does not offer the fluorescence intensity of Cy5.5. The approval of a fluorescent marker that provides intense fluorescence, although

posing no toxic hazard to the patient, is imperative to facilitate clinical experimentation. It is possible that background fluorescence in a human would be higher because mice do not express human EGFR. However, previous studies using the technique on human skin grafts did not demonstrate any detectable fluorescence.[8] Because this was a pilot study to demonstrate the feasibility of the imaging technique for detection of metastasis, a relatively small number of mice were used.

We provide evidence that fluorescent-guided neoplasm detection can be used to identify micrometastatic disease in the cervical lymph nodes and the lungs. Importantly, we have also shown the utility of fluorescence in the guided removal of tumors that are too small to be detected by gross palpation (<1 mm). Because understanding the extent of disease in these areas is crucial to therapy and staging, this technique might be worth pursuing in the clinical setting.

Acknowledgments

Contract grant sponsor: American Cancer Society; contract grant number: RSG-06-1006-01-CCE; contract grant sponsor: National Cancer Institute; contract grant number: NCI K08CA102154; contract grant sponsor: Synthes CMF.

REFERENCES

1. Som PM. Detection of metastasis in cervical lymph nodes: CT and MR criteria and differential diagnosis. Am J Roentgenol. 1992; 158:961–969. [PubMed: 1566697]
2. Lardinois D, Weder W, Hany TF, et al. Staging of nonsmall-cell lung cancer with integrated positron-emission tomography and computed tomography. N Engl J Med. 2003; 348:2500–2507. [PubMed: 12815135]
3. Veiseh M, Gabikian P, Bahrami SB, et al. Tumor paint: a chlorotoxin:Cy5.5 bioconjugate for intraoperative visualization of cancer foci. Cancer Res. 2007; 67:6882–6888. [PubMed: 17638899]
4. Koyama Y, Hama Y, Urano Y, Nguyen DM, Choyke PL, Kobayashi H. Spectral fluorescence molecular imaging of lung metastases targeting HER2/neu. Clin Cancer Res. 2007; 13:2936–2945. [PubMed: 17504994]
5. Pomerantz RG, Grandis JR. The role of epidermal growth factor receptor in head and neck squamous cell carcinoma. Curr Oncol Rep. 2003; 5:140–146. [PubMed: 12583831]
6. Shin DM, Ro JY, Hong WK, Hittelman WN. Dysregulation of epidermal growth factor receptor expression in premalignant lesions during head and neck tumorigenesis. Cancer Res. 1994; 54:3153–3159. [PubMed: 8205534]
7. Bonner JA, Harari PM, Giralt J, et al. Radiotherapy plus cetuximab for squamous-cell carcinoma of the head and neck. N Engl J Med. 2006; 354:567–578. [PubMed: 16467544]
8. Rosenthal EL, Kulbersh BD, King T, Chaudhuri TR, Zinn KR. Use of fluorescent labeled anti-epidermal growth factor receptor antibody to image head and neck squamous cell carcinoma xenografts. Mol Cancer Ther. 2007; 6:1230–1238. [PubMed: 17431103]
9. Rosenthal EL, Kulbersh BD, Duncan RD, et al. In vivo detection of head and neck cancer orthotopic xenografts by immunofluorescence. Laryngoscope. 2006; 116:1636–1641. [PubMed: 16954995]
10. Kulbersh BD, Duncan RD, Magnuson JS, Skipper JB, Zinn K, Rosenthal EL. Sensitivity and specificity of fluorescent immunoguided neoplasm detection in head and neck cancer xenografts. Arch Otolaryngol Head Neck Surg. 2007; 133:511–515. [PubMed: 17520766]
11. Maekawa K, Sato H, Furukawa M, Yoshizaki T. Inhibition of cervical lymph node metastasis by marimastat (BB-2516) in an orthotopic oral squamous cell carcinoma implantation model. Clin Exp Metastasis. 2002; 19:513–518. [PubMed: 12405288]

12. Folli S, Westermann P, Braichotte D, et al. Antibody-indocyanin conjugates for immunophotodetection of human squamous cell carcinoma in nude mice. Cancer Res. 1994; 54:2643–2649. [PubMed: 8168092]
13. Goldenberg A, Masui H, Divgi C, Kamrath H, Pentlow K, Mendelsohn J. Imaging of human tumor xenografts with an indium-111-labeled anti-epidermal growth factor receptor monoclonal antibody. J Natl Cancer Inst. 1989; 81:1616–1625. [PubMed: 2795690]
14. Weissleder R, Tung CH, Mahmood U, Bogdanov A Jr. In vivo imaging of tumors with protease-activated near-infrared fluorescent probes. Nat Biotechnol. 1999; 17:375–378. [PubMed: 10207887]
15. Nimura H, Narimiya N, Mitsumori N, Yamazaki Y, Yanaga K, Urashima M. Infrared ray electronic endoscopy combined with indocyanine green injection for detection of sentinel nodes of patients with gastric cancer. Br J Surg. 2004; 91:575–579. [PubMed: 15122608]
16. Soltesz EG, Kim S, Kim SW, et al. Sentinel lymph node mapping of the gastrointestinal tract by using invisible light. Ann Surg Oncol. 2006; 13:386–396. [PubMed: 16485157]
17. Parungo CP, Ohnishi S, Kim SW, et al. Intraoperative identification of esophageal sentinel lymph nodes with near-infrared fluorescence imaging. J Thorac Cardiovasc Surg. 2005; 129:844–850. [PubMed: 15821653]
18. Ito N, Fukuta M, Tokushima T, Nakai K, Ohgi S. Sentinel node navigation surgery using indocyanine green in patients with lung cancer. Surg Today. 2004; 34:581–585. [PubMed: 15221551]
19. Tanaka E, Choi HS, Fujii H, Bawendi MG, Frangioni JV. Image-guided oncologic surgery using invisible light: completed pre-clinical development for sentinel lymph node mapping. Ann Surg Oncol. 2006; 13:1671–1681. [PubMed: 17009138]
20. Asgari S, Rohrborn HJ, Engelhorn T, Stolke D. Intraoperative characterization of gliomas by near-infrared spectroscopy: possible association with prognosis. Acta Neurochir (Wien). 2003; 145:453–459. Discussion 459–460. [PubMed: 12836069]
21. Kircher MF, Mahmood U, King RS, Weissleder R, Josephson L. A multimodal nanoparticle for preoperative magnetic resonance imaging and intraoperative optical brain tumor delineation. Cancer Res. 2003; 63:8122–8125. [PubMed: 14678964]
22. Stummer W, Pichlmeier U, Meinel T, Wiestler OD, Zanella F, Reulen HJ. Fluorescence-guided surgery with 5-aminolevulinic acid for resection of malignant glioma: a randomised controlled multicentre phase III trial. Lancet Oncol. 2006; 7:392–401. [PubMed: 16648043]
23. Sokolov K, Follen M, Aaron J, et al. Real-time vital optical imaging of precancer using anti-epidermal growth factor receptor antibodies conjugated to gold nanoparticles. Cancer Res. 2003; 63:1999–2004. [PubMed: 12727808]
24. Nida DL, Rahman MS, Carlson KD, Richards-Kortum R, Follen M. Fluorescent nanocrystals for use in early cervical cancer detection. Gynecol Oncol. 2005; 99:S89–S94. [PubMed: 16139342]

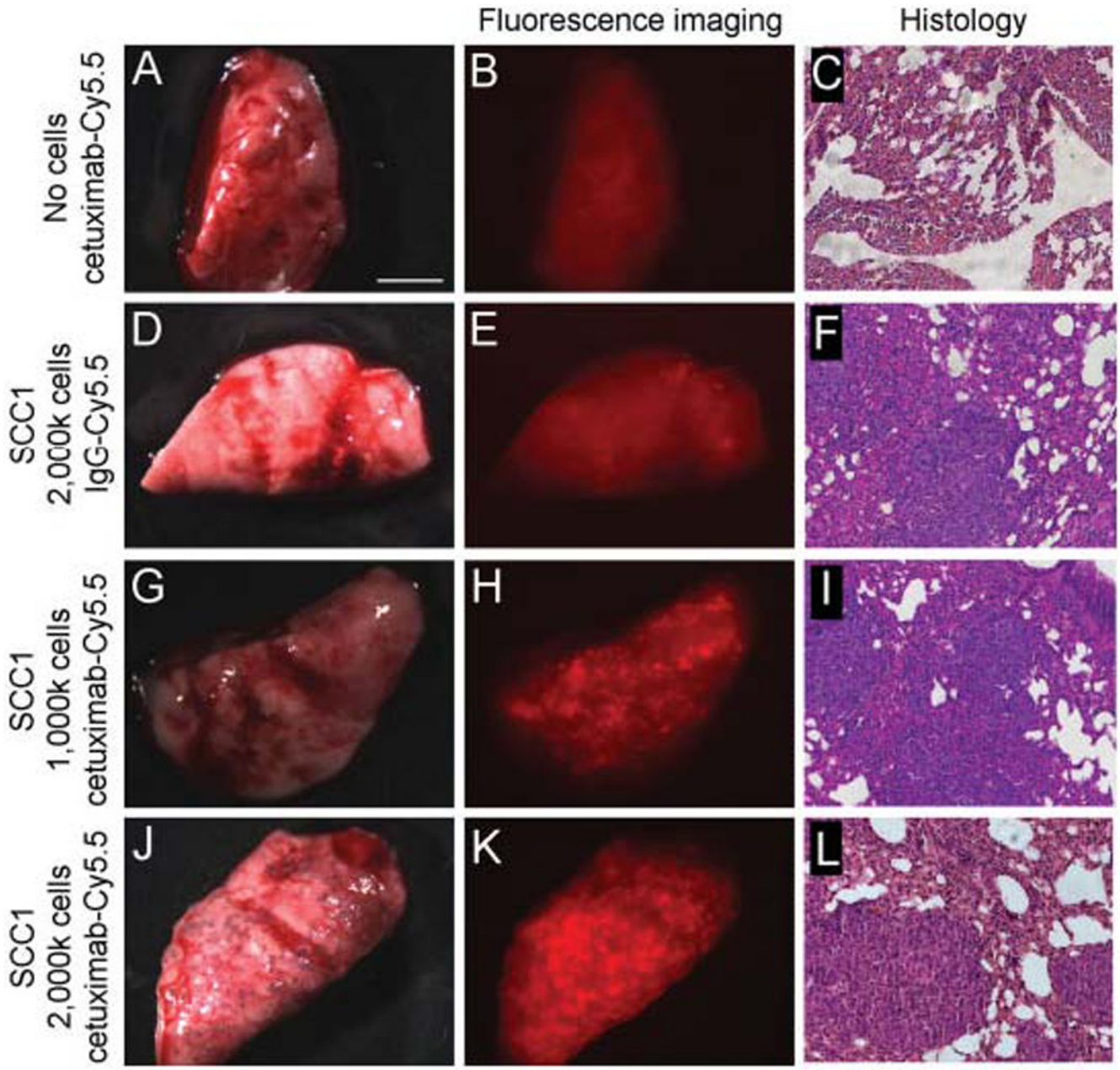

FIGURE 1.

Cetuximab–Cy5.5 detects pulmonary metastasis in vivo. Injection of the cetuximab–Cy5.5 fluorescent bioconjugate alone in the absence of tumor cells (**A–C**) demonstrates some diffuse background after fluorescent imaging. Pulmonary metastases are formed after injection of 1×10^6 (**D–I**) or 2×10^6 SCC1 cells (**J–L**). Injection of nonspecific IgG1–Cy5.5 bioconjugate in mice bearing pulmonary metastases (D–F) does not demonstrate significant fluorescence after stereomicroscopic imaging. However, when mice bearing 1×10^6 (G–I) or 2×10^6 SCC1 cells (J–L) were administered cetuximab–Cy5.5, a distinctive miliary pattern of fluorescence was seen and tumor micrometastases were confirmed by pathology. Bar = 5 mm.

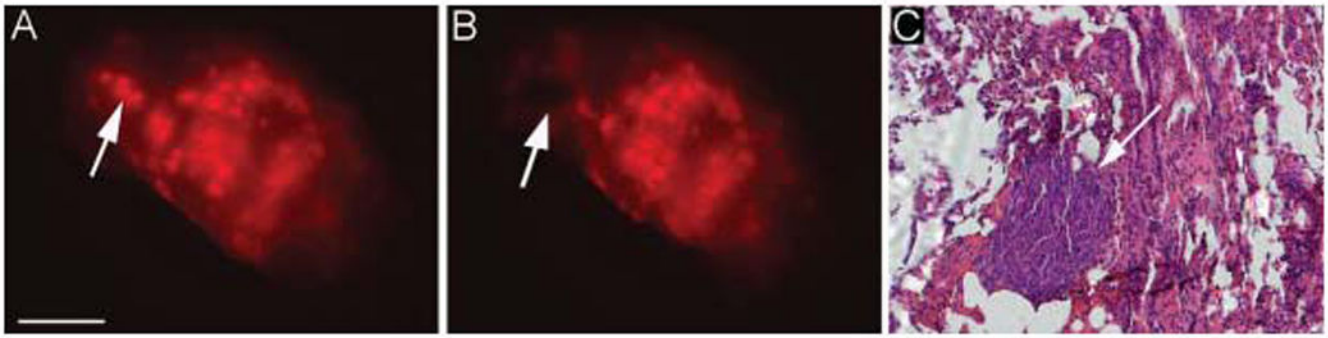

FIGURE 2.

Fluorescent spots correlate to tumor micrometastasis. Biopsy of 2-mm fluorescent dot coincides with presence of micrometastatic disease as confirmed by pathology. Bar = 5 mm. [Color figure can be viewed in the online issue, which is available at www.interscience.wiley.com.]

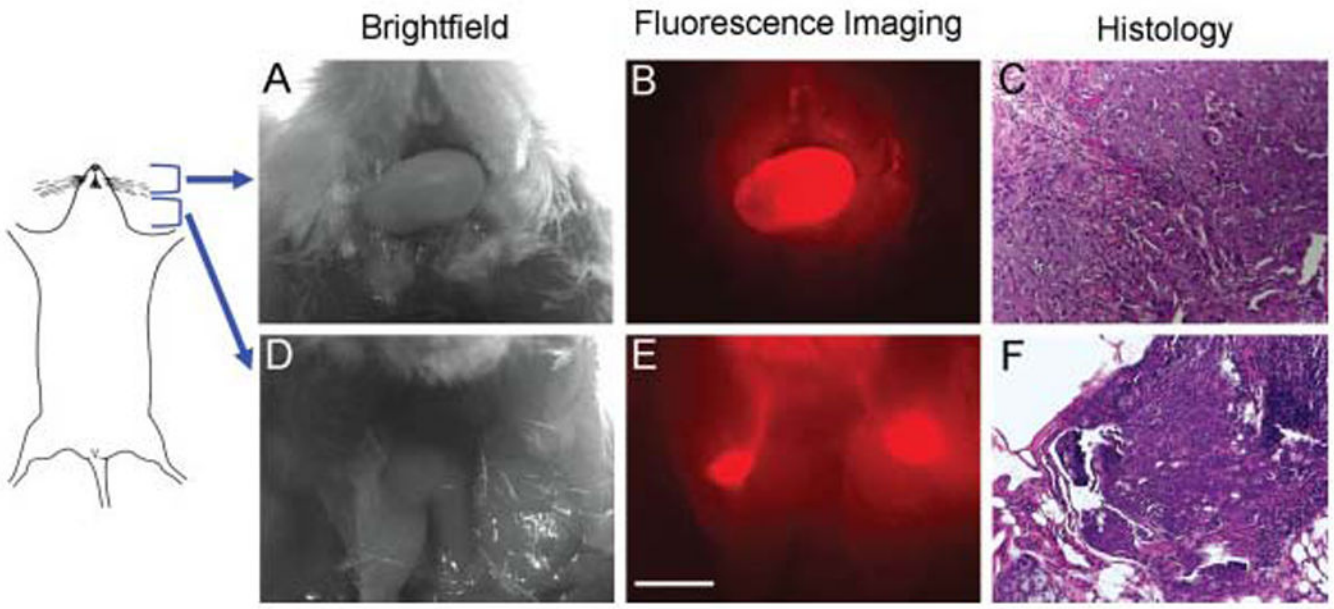

FIGURE 3.

Cervical metastases in an orthotopic murine model were detected with systemically injected cetuximab–Cy5.5 conjugate. The primary tongue tumor (**A**–**C**) was clearly visualized under fluorescent imaging after systemic injection of cetuximab–Cy5.5. After removal of cervical skin, bilateral draining lymph nodes could be identified and confirmed by pathology. Bar = 2 mm.

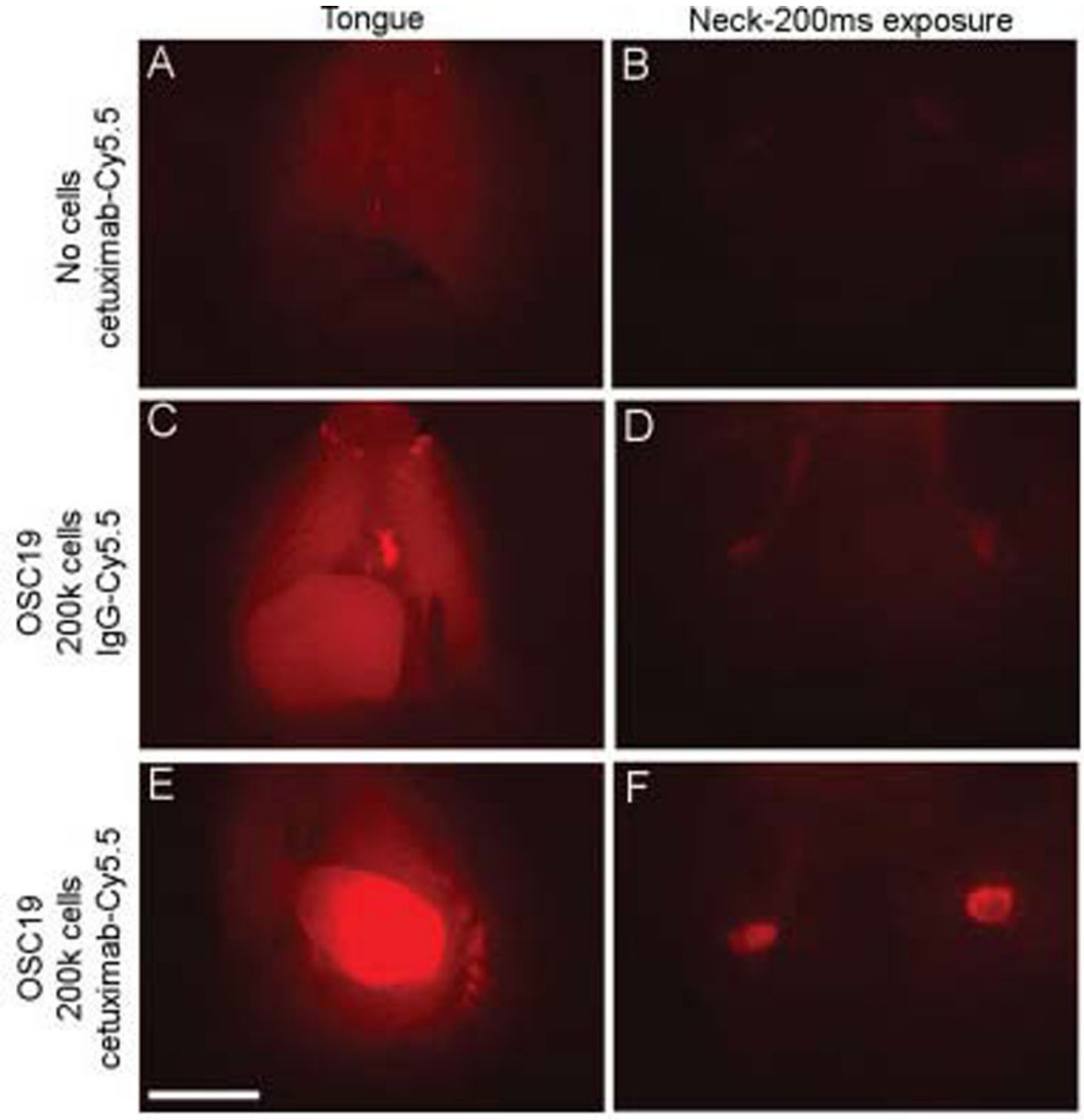

FIGURE 4.

Most intense lymph node fluorescence is seen as a result of specific binding. Injection of the cetuximab–Cy5.5 conjugate alone in the absence of tumor cells (**A, B**) demonstrates very little background fluorescence after stereomicroscopic imaging. Mice bearing primary and metastatic OSC19 tumors display diffuse fluorescence after injection of labeled isotype control IgG1–Cy5.5 (**C, D**). Fluorescent imaging after injection of specific cetuximab–Cy5.5 conjugate allows excellent visualization of clearly circumscribed tumors, both primary and metastatic (**E, F**). The difference in fluorescence intensity between the 3 groups

of lymph nodes was measured and found to be very statistically significant ($p = .0005$). Bar = 2 mm. [Color figure can be viewed in the online issue, which is available at www.interscience.wiley.com.]

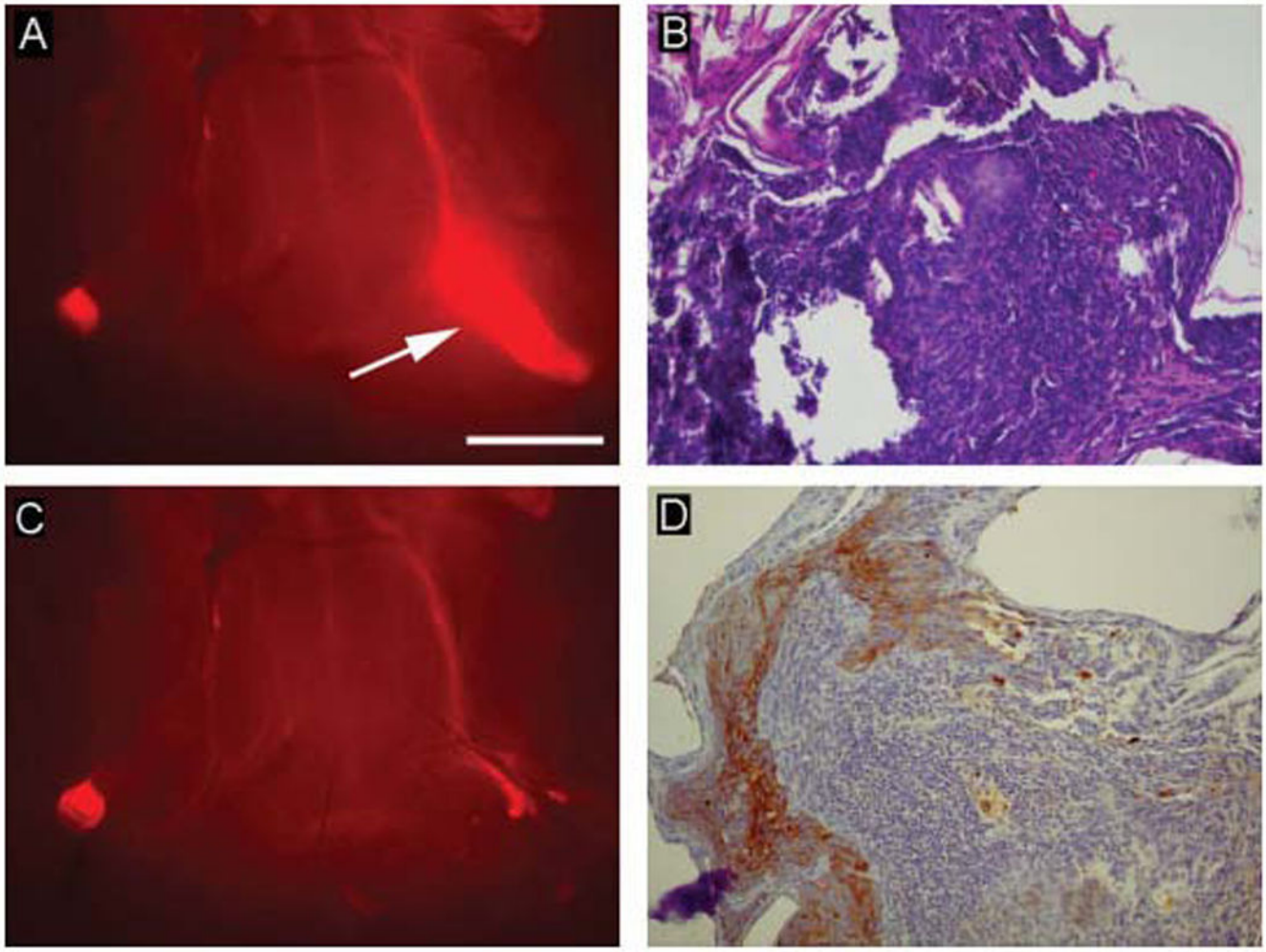

FIGURE 5.

Systemic injection of cetuximab–Cy5.5 conjugate enables fluorescence-guided surgical lymph node resection. Fluorescent areas were excised until fluorescence disappeared (**A, C**). Although tumor is not entirely clear on the hematoxylin-eosin (H&E) stain (**B**), due to artifact from crushing during handling of the specimen, immunohistochemical staining using cytokeratin AE1 antibody (**D**) emphasizes pathologic epithelial tissue within the lymph node. Only 1 node resection is shown. Bar = 2 mm.